Removing Effects of Parallel Capacitances from Inductance and Resistance Measurements

Bryce Hesterman

Utah State University – ASPIRE
bryce@ieee.org
Rev 1 5/12/2025

UtahStateUniversity

ASPIRE
NSF Engineering Research Center

IS17.6

Overview

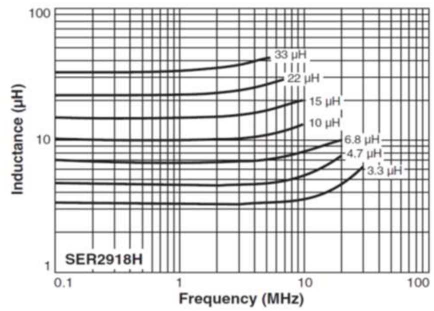

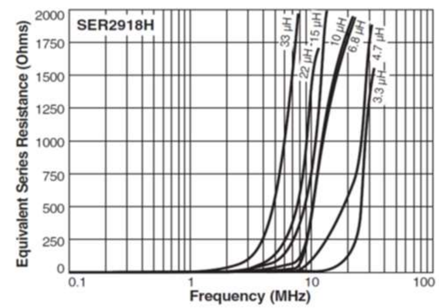

- Inductor datasheets commonly show inductance increasing with frequency, but this is actually an effect caused by parallel capacitance
- This issue was raised by Dr. Ray Ridley
- This presentation proposes a method of compensating for the capacitive effects to more accurately determine the inductance and resistance values

Example Capacitive Correction

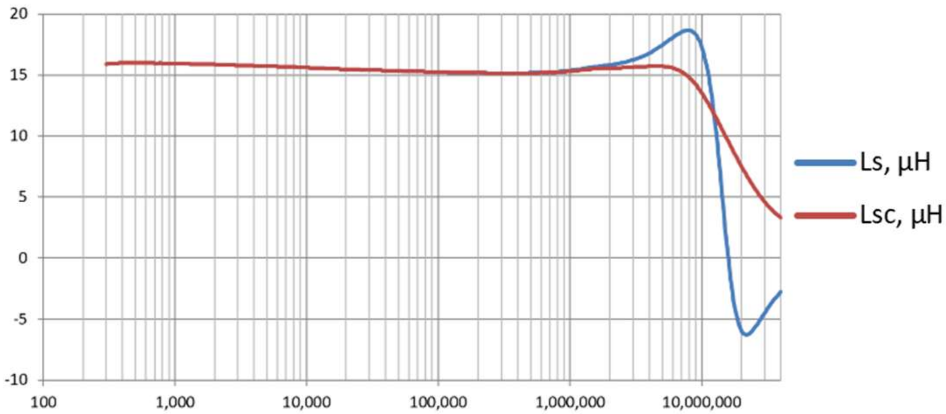

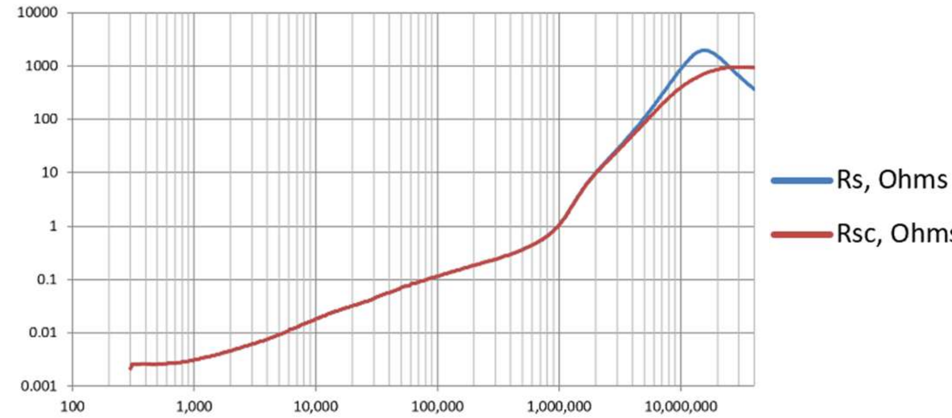

- Inductance and resistance measurements were made on a Coilcraft 15 µH SER2918H-153 inductor with an HP4194A network analyzer
- Corrections to Ls and Rs were made using the proposed method resulting in the corrected values Lsc and Rsc

Steps of the Correction Method

- The series inductances and series resistances are measured over a range of frequencies and then converted to series reactances and series resistances
- The parallel capacitance is identified by analyzing the measured data, and it is assumed to be constant
- For each measured datapoint, the series impedances are converted to the equivalent parallel form
- The effects of the parallel capacitance are removed
- The corrected parallel impedance data is converted back to the series form and then the series reactances are converted to series inductances
- Parallel capacitance can be added to RL circuit models

Parallel Capacitance Identification

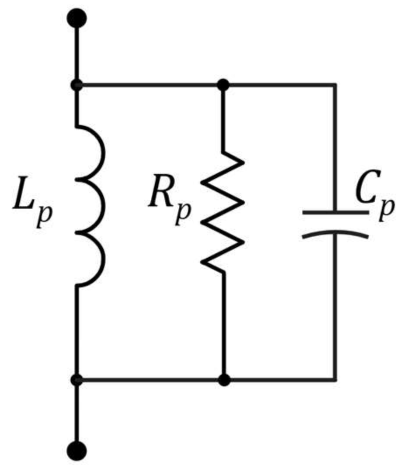

$$\omega = 2\pi f \qquad X_{Cp} = \frac{1}{\omega C_p}$$

- The HP4194A network analyzer calculated equivalent circuit values from measured impedance data, but other methods are discussed later in the presentation
- The parallel capacitance value is used in the corrections

Series-Parallel Transformation

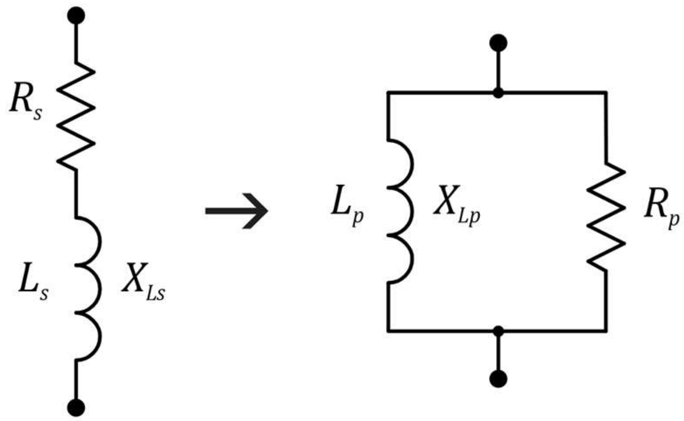

$$X_p = \frac{{X_s}^2 + {R_s}^2}{X_s} \qquad R_p = \frac{{X_s}^2 + {R_s}^2}{R_s}$$

- The transformations are valid at one frequency
- The series reactance and series resistance are converted to the equivalent parallel form for each measured frequency

Capacitance Correction

$$X_{Lpc} = \frac{1}{\frac{1}{X_{Lp}} - \frac{1}{X_{Cp}}}$$

- The corrected parallel reactance value is determined by using the subtractive form of the parallel impedance formula

Parallel-Series Transformation

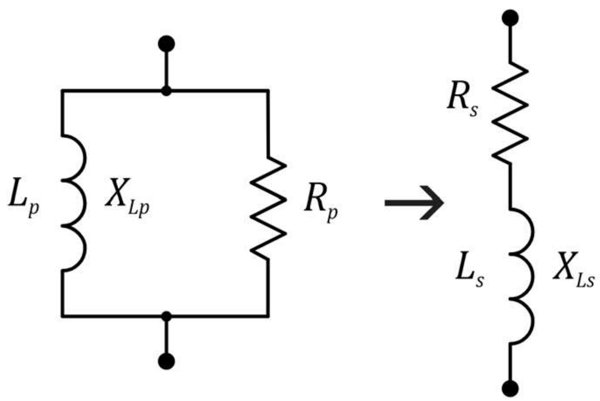

$$X_s = \frac{{R_p}^2 X_p}{{X_p}^2 + {R_p}^2} \qquad R_s = \frac{R_p {X_p}^2}{{X_p}^2 + {R_p}^2}$$

$$\downarrow \qquad\qquad \downarrow$$

$$X_{Lsc} = \frac{{R_p}^2 X_{Lpc}}{{X_{Lpc}}^2 + {R_p}^2} \qquad R_{sc} = \frac{R_p {X_{Lpc}}^2}{{X_{Lpc}}^2 + {R_p}^2}$$

- The corrected parallel reactances and resistances are converted back to the equivalent series form for each measured frequency and the series reactance is converted to series inductance

Parallel Capacitor Added

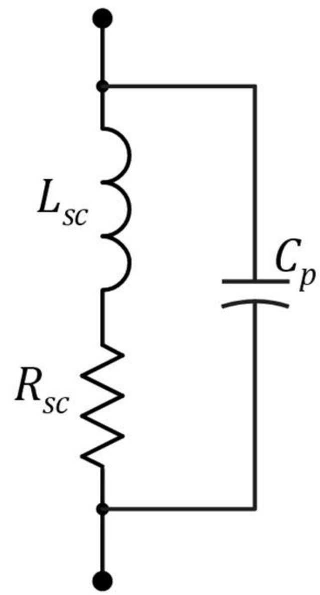

- The parallel capacitance used in the corrections can be added back into an RL circuit model to make an RLC model

2nd Example of Capacitive Correction

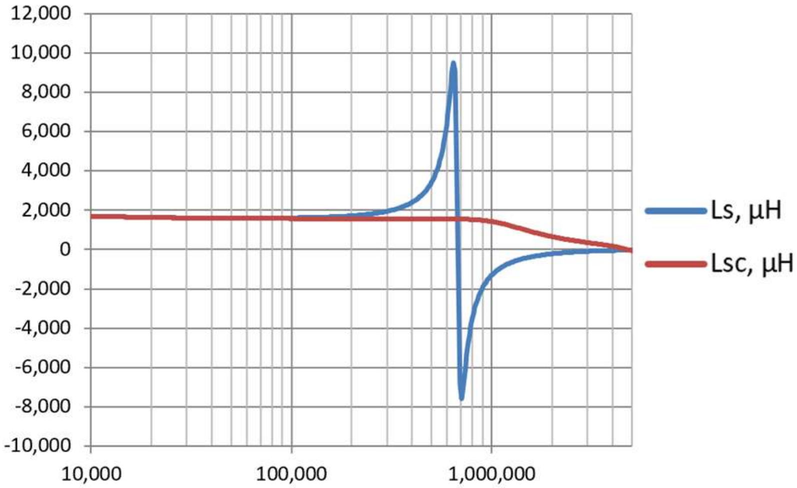

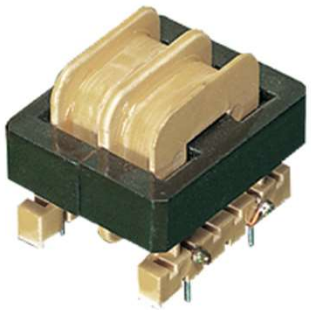

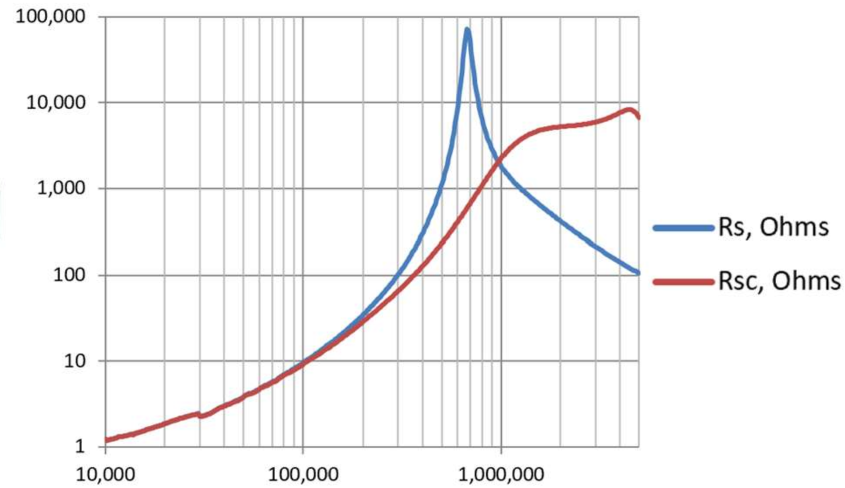

- The method also works for multi-winding magnetics
- Coilcraft F5593-AL high-impedance common-mode choke
- The corrected data extends the frequency range for accurate L-R measurements by almost a decade
- Multiple resonances are typical, but only the first resonance is corrected

Extracting the Low-frequency Inductance

$$Freq_0 = 10\ \mathbf{kHz} \qquad Freq_{10} = 12.3\ \mathbf{kHz}$$

$$L_{p\_ini} := \frac{MagZ_{10} - MagZ_0}{2 \cdot \pi \cdot \left(Freq_{10} - Freq_0\right)} = 15.16\ \mu H$$

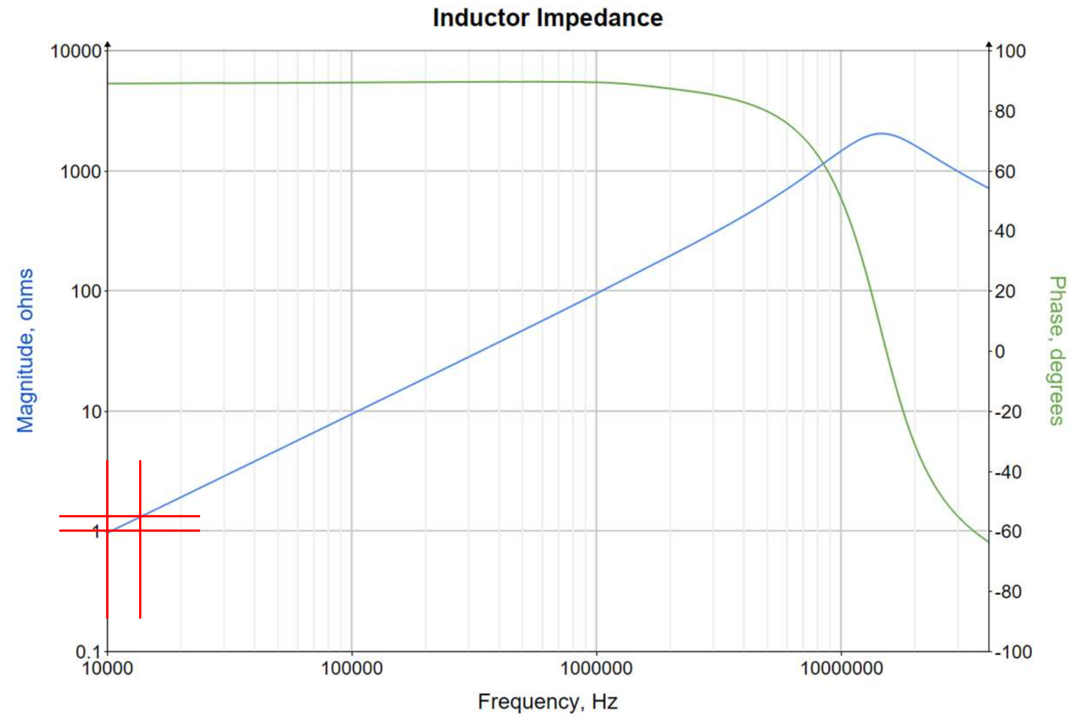

- The low-frequency inductance can be determined from the initial slope of the impedance plot [4] or by direct measurement

Extracting the Parallel Capacitance

$$C_p = \frac{1}{(2\pi f_0)^2 L_p}$$

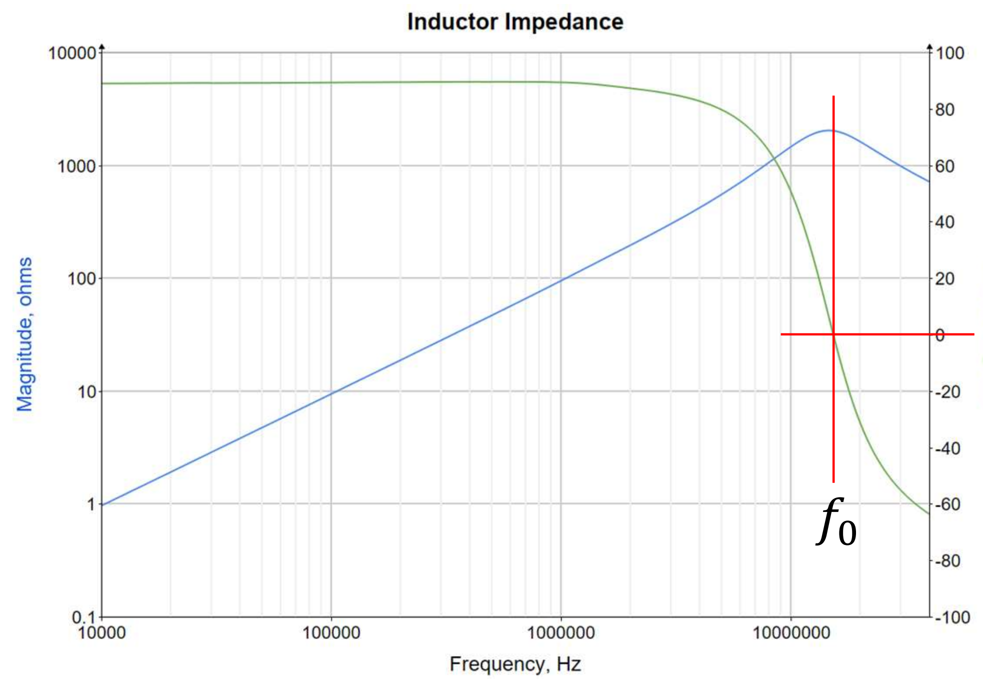

- The parallel capacitance can be determined from the resonant frequency f_0 and the low-frequency inductance
- See [9] for other methods of determining the parallel capacitance

Extracting the Parallel Resistance

- The peak of the impedance curve occurs slightly below resonance due to inductor losses that could be modeled as a series resistance

$$R_p = |Z_o|$$

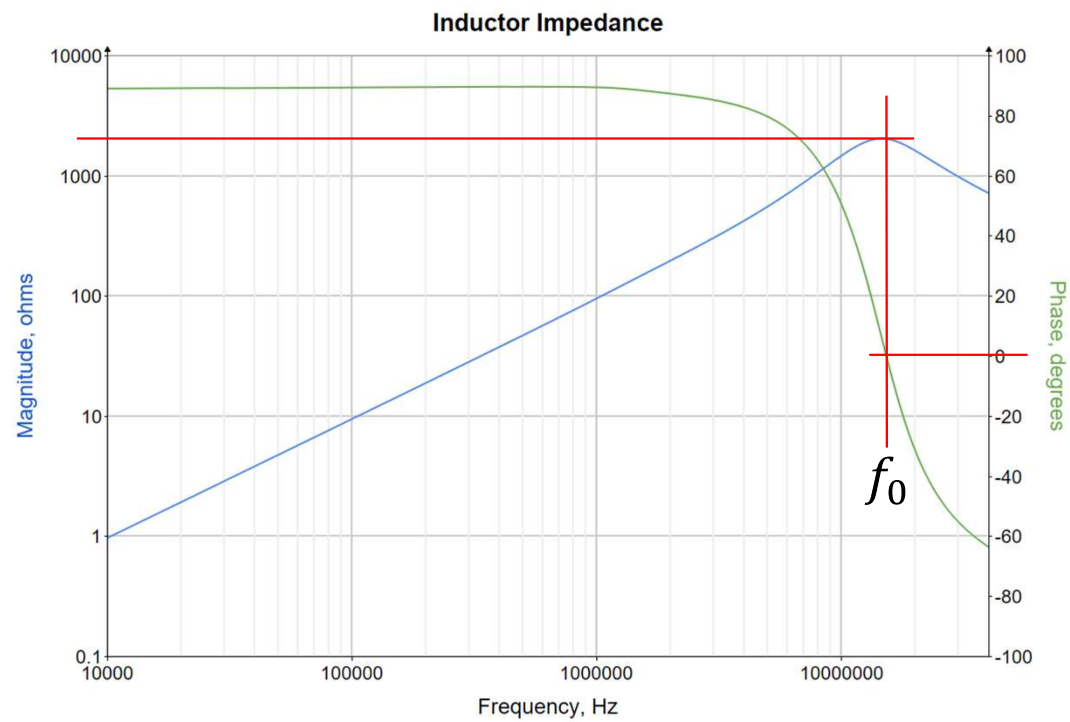

- The parallel resistance can be determined from the magnitude of the impedance at the resonant frequency f_0

Extracting RLC Values Using a Mathcad Solver

Impedance Magnitude

$$MagZ_{eq}\left(L_p, C_p, R_p, f\right) := \left|\frac{1}{\frac{1}{1j \cdot 2 \cdot \pi \cdot f \cdot L_p} + 1j \cdot 2 \cdot \pi \cdot f \cdot C_p + \frac{1}{R_p}}\right|$$

Impedance Phase

$$Phase_{eq}\left(L_p, C_p, R_p, f\right) := \arg\left(\frac{1}{\frac{1}{1j \cdot 2 \cdot \pi \cdot f \cdot L_p} + 1j \cdot 2 \cdot \pi \cdot f \cdot C_p + \frac{1}{R_p}}\right) \cdot \frac{1}{deg}$$

- Functions are defined for the impedance magnitude and phase in terms of the component values and frequency

Error Functions for the Mathcad Solver

Magnitude Error

$$Error_{mag}\left(L_p, C_p, R_p, n\right) := \frac{MagZ_{eq}\left(L_p, C_p, R_p, Freq_n\right) - MagZ_n}{MagZ_n}$$

Phase Error

$$Error_{phase}\left(L_p, C_p, R_p, n\right) := \left|\frac{Phase_{eq}\left(L_p, C_p, R_p, Freq_n\right) - Phase_n}{Phase_n} + 1\right|$$

- Normalized functions are defined for the errors between impedance magnitude and phase and the measured data

Error Function Responses at f_0

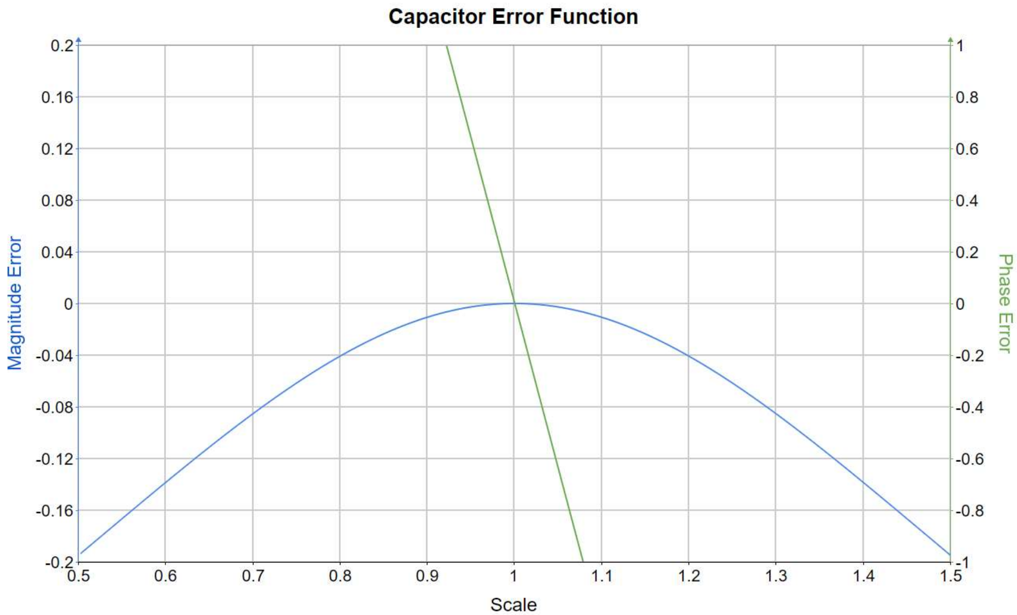

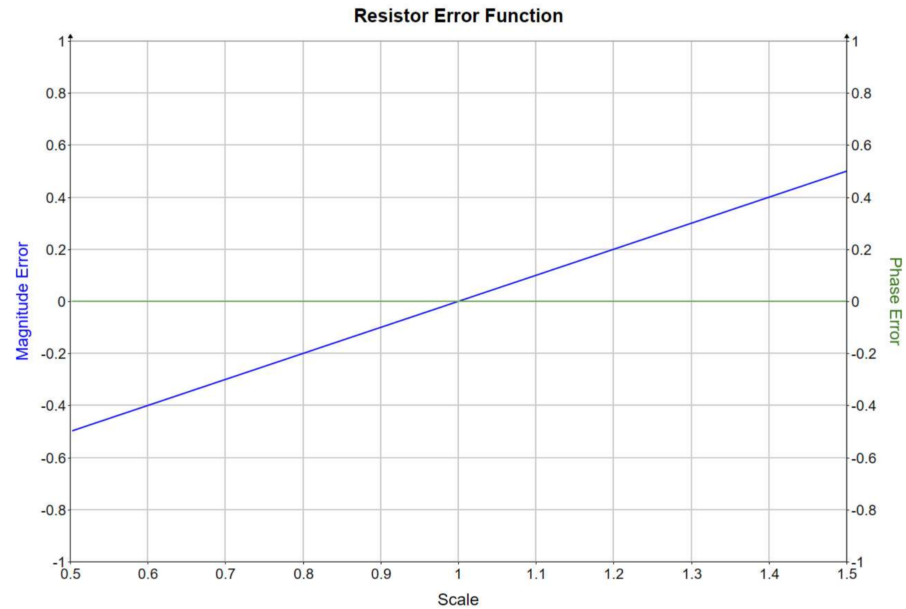

- The capacitor and resistor were varied from 50% to 150% of the known values to examine the error function response
- The resistor scaling doesn't produce phase error at f_0

APEC2025

Mathcad Minerr Solver

Guess Values

$$C_p := 0.5 \cdot C_{p\_ini} \qquad R_p := 0.5 \cdot R_{p\_ini}$$

Constraints

$$Error_{mag}\left(L_{p\_ini}, C_p, R_p, MaxRow\right) = 0$$

$$Error_{phase}\left(L_{p\_ini}, C_p, R_p, MaxRow\right) = 0$$

Solver

$$\begin{bmatrix} C_{p\_opt} \\ R_{p\_opt} \end{bmatrix} := \mathbf{Minerr}\left(C_p, R_p\right)$$

Optimized Values

$$C_{p\_opt} = 7.97\ pF \qquad R_{p\_opt} = 2.03\ k\Omega$$

- The Minerr solver minimizes the error by adjusting the values of R_p and C_p using a Levenberg-Marquardt algorithm

Solver Operating Point

Guess Values

$$C_p := 0.5 \cdot C_{p\_ini} \qquad R_p := 0.5 \cdot R_{p\_ini}$$

Constraints

$$Error_{mag}\left(L_{p\_ini}, C_p, R_p, MaxRow\right) = 0$$

$$Error_{phase}\left(L_{p\_ini}, C_p, R_p, MaxRow\right) = 0$$

Solver

$$\begin{bmatrix} C_{p\_opt} \\ R_{p\_opt} \end{bmatrix} := \mathbf{Minerr}\left(C_p, R_p\right)$$

Optimized Values

$$C_{p\_opt} = 7.97\ pF \qquad R_{p\_opt} = 2.03\ k\Omega$$

- The error functions are set to operate at the highest value of the impedance magnitude in the measured data set which may or may not include the resonant frequency
- The correction capacitance can be calculated by using the low-frequency L, and L and R values at a higher frequency

Extracting RLC Values Below Resonance

With peak of Z_{mag}

$$C_{p\_opt} = 7.35\ pF \qquad R_{p\_opt} = 2.05\ \mathbf{k\Omega}$$

Without peak of Z_{mag}

$$C_{p\_opt} = 7.60\ \mathbf{pF} \qquad R_{p\_opt} = 2.10\ \mathbf{k\Omega}$$

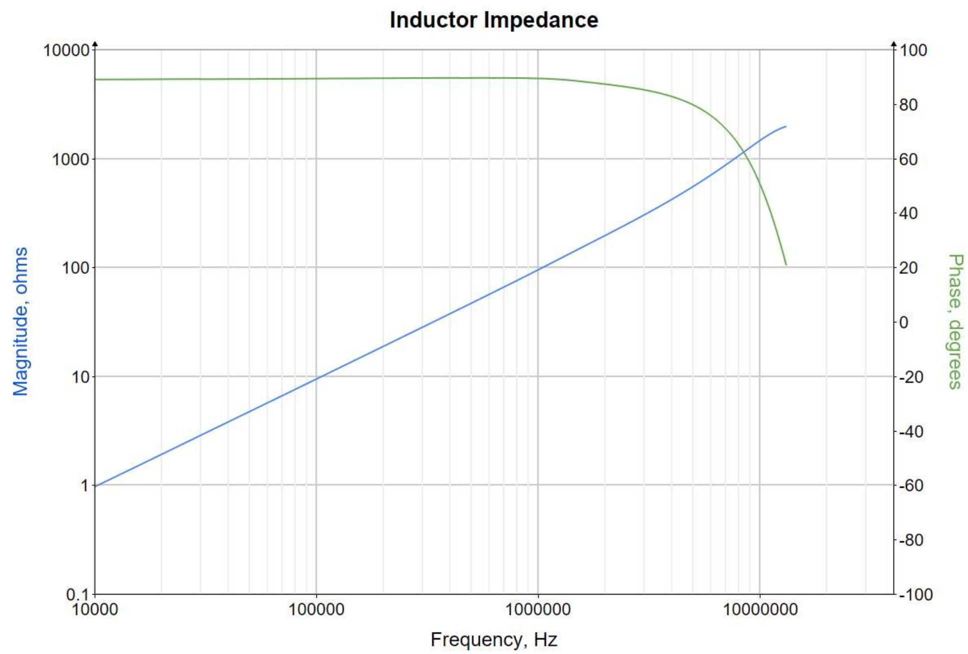

- The solver gives reasonably good results even if the peak value of the impedance isn't included in the data set

Common Equivalent Circuits

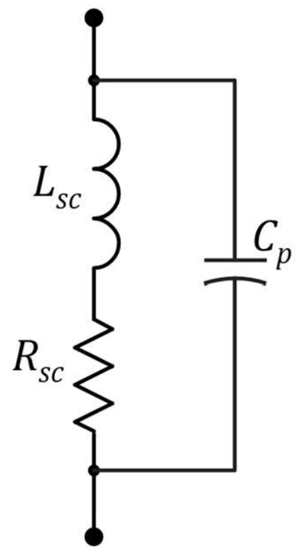

Simple RLC model

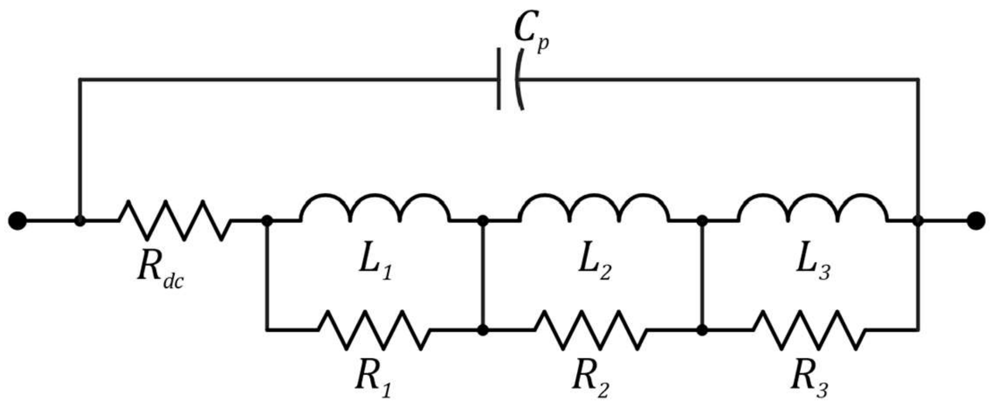

Type 1 Foster Network RL model with added parallel capacitor

- A Foster Network can be used to extend the valid frequency range compared to a simple RLC model [5, 6]
- More complicated models have also been developed [7]

Conclusions

- The proposed correction method improves the accuracy of inductance measurements thereby enabling the generation of more accurate wideband equivalent circuit models of magnetic devices based on measured data
- The method also enables producing more accurate datasheet plots for commercial magnetics
- RLC values can be derived from measured impedance data even if the peak impedance isn’t in the data set
- The method also works for multi-winding magnetics

References

1. A. F. Jaimes, F. L. Cabrera and F. R. de Sousa, "Characterization of High-Q Inductors Up to its Self-Resonance Frequency for Wireless Power Transfer Applications," in IEEE Microwave and Wireless Components Letters, vol. 28, no. 12, pp. 1071-1073, Dec. 2018, doi: 10.1109/LMWC.2018.2876770.
2. T. Ohira, "What in the World Is Q? [Distinguished Microwave Lecture]," in IEEE Microwave Magazine, vol. 17, no. 6, pp. 42-49, June 2016, doi: 10.1109/MMM.2016.2538512.
3. W. B. Kuhn and A. P. Boutz, "Measuring and Reporting High Quality Factors of Inductors Using Vector Network Analyzers," in IEEE Transactions on Microwave Theory and Techniques, vol. 58, no. 4, pp. 1046-1055, April 2010, doi: 10.1109/TMTT.2010.2042843.
4. P. A. Kyaw, "Deriving Loss Models from Measurements," PSMA High Frequency Magnetics Workshop, June 9, 2020. https://www.psma.com/technical-forums/magnetics/presentations
5. F. de Leon and A. Semlyen, "Time domain modeling of eddy current effects for transformer transients," in IEEE Transactions on Power Delivery, vol. 8, no. 1, pp. 271-280, Jan. 1993, doi: 10.1109/61.180346.
6. H. Zhu, D. Liu, H. Chen and G. Chen, "An improved foster model of common-mode inductor and its application in EMI filter design," 2018 IEEE International Symposium on Electromagnetic Compatibility and 2018 IEEE Asia-Pacific Symposium on Electromagnetic Compatibility (EMC/APEMC), Suntec City, Singapore, 2018, pp. 461-465, doi: 10.1109/ISEMC.2018.8393821.
7. N. Moonen, J. L. Rotgerink and F. Leferink, "Automated equivalent circuit extraction of impedance curves using a Gauss-Newton algorithm," 2018 IEEE International Symposium on Electromagnetic Compatibility and 2018 IEEE Asia-Pacific Symposium on Electromagnetic Compatibility (EMC/APEMC), Suntec City, Singapore, 2018, pp. 1103-1108, doi: 10.1109/ISEMC.2018.8393958.
8. Standard IEC 61007:2020 (4.4.6.1 Self-capacitance, Procedure 2)
9. https://www.verimod.com/pdf_files/SER2918H-153_Corrected_Inductance.xlsx

Bryce Hesterman

Utah State University – ASPIRE

bryce@ieee.org